Role of vibrationally excited HBr in a HBr/He inductively coupled plasma used for etching of silicon

Reference:

Tinck Stefan, Bogaerts Annemie.- Role of vibrationally excited HBr in a HBr/He inductively coupled plasma used for etching of silicon

Journal of physics: D: applied physics - ISSN 0022-3727 - 49:24(2016), p. 1-6

Full text (Publishers DOI): http://dx.doi.org/doi:10.1088/0022-3727/49/24/245204

Role of vibrationally excited HBr in a HBr/He inductively coupled plasma used for etching of silicon

Stefan Tinck and Annemie Bogaerts

Research Group PLASMANT, Dept. of Chemistry, University of Antwerp, Universiteitsplein 1, B-2610 Antwerp, Belgium

Abstract.

In this work, the role of vibrationally excited HBr ($HBr^{(vib)}$) is computationally investigated for a HBr/He inductively coupled plasma applied for Si etching. It is found that at least 50% of all dissociations of HBr occur through $HBr^{(vib)}$. This additional dissociation pathway through $HBr^{(vib)}$ makes the plasma significantly more atomic. It also results in a slightly higher electron temperature (i.e., about 0.2 eV higher compared to simulation results where $HBr^{(vib)}$ is not included), as well as a higher gas temperature (i.e., about 50 K higher than without including $HBr^{(vib)}$), due to the enhanced Franck-Condon heating through $HBr^{(vib)}$ dissociation, at the conditions investigated. Most importantly, the calculated etch rate with $HBr^{(vib)}$ included in the model is a factor 3 higher than in the case without $HBr^{(vib)}$, due to the higher fluxes of etching species (i.e., H and Br), while the chemical composition of the wafer surface shows no significant difference. Our calculations clearly show the importance of including $HBr^{(vib)}$ for accurate modeling of HBr-containing plasmas.

1. Introduction

In recent years, bromine-containing plasmas have seen an increase in popularity in microelectronics development due to the shrinking ultra-small scale components found in modern integrated circuits. Because of the lower reactivity of bromine towards silicon compared to fluorine, the etching of very thin layers can be more properly controlled with bromine-based plasmas.[1-7] A bromine-containing gas that is often used for silicon etching is HBr, which is commonly mixed with Cl_2 and/or CF_4.[8-13] Furthermore, HBr can also be combined with a noble gas like helium, to tune the ratio between

physical ion sputtering and chemical etching, or with O_2, for controlling the anisotropy during etching.[14-17]

Since HBr is a polar molecule, the vibrational excitation cross sections are typically very large, and a significant fraction of HBr is believed to be in vibrational states.[18] Moreover, electron impact dissociative attachment on vibrationally excited HBr - denoted in this paper as $HBr^{(vib)}$ - happens more than 10 times easier than on ground state HBr, which is a well-known effect observed for all hydrogen halides.[19] This is clear from **Figure 1,** which illustrates the cross sections for three electron impact vibrational excitations of HBr, as well as those for dissociative attachment on both ground state HBr and $HBr^{(vib)}$.

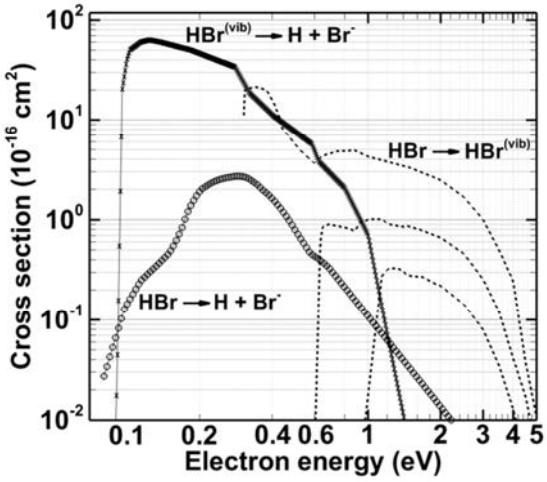

Figure 1. Cross sections as a function of electron energy for three electron impact vibrational excitations of HBr, obtained from reference[5] (dashed lines), as well as for dissociative attachment on ground state HBr (circle symbols) and on $HBr^{(vib)}$ (cross symbols), obtained from reference[6]. Please note that both X and Y axes have logarithmic scales for clarity.

The electron impact dissociative attachment cross section on $HBr^{(vib)}$ is more than an order of magnitude larger and has a maximum at lower electron energy (~0.1 eV) than the cross section on ground state HBr (~0.3 eV). However, for dissociative attachment of $HBr^{(vib)}$ to happen, ground state HBr must first be vibrationally excited, which comprises two successive electron impact reactions, compared to only one reaction when ground state HBr is dissociated directly into H and Br^-.

In an inductively coupled plasma (ICP) used for the etching of silicon, at typical operating conditions, the electrons usually have a (near)-Maxwellian rf cycle averaged energy distribution,

ranging roughly from 0 eV to 30 eV, although this is strongly dependent on gas type, power, pressure and operating frequency.[20] As a result, it can be expected that a significant fraction of HBr is vibrationally excited in the plasma. Nevertheless, these vibrationally excited species are sometimes neglected in computer simulations for the sake of simplicity.[21,22] In the present paper, we investigate the importance of $HBr^{(vib)}$ in the plasma, for an ICP operating in HBr/He, by performing simulations with and without including $HBr^{(vib)}$. More specifically, we will study its influence on the most important plasma properties like plasma density, electron temperature and gas temperature, as well as on the etch rate.

2. Computational details

We make use of a two-dimensional hybrid Monte Carlo - fluid model, called HPEM and developed by Kushner.[23] A detailed explanation of this model can be found in the reference, but a brief description follows here. For calculating the plasma characteristics, the model uses three modules. After defining the reactor geometry and initial operating conditions, the first module, called the Electromagnetics Module (EMM), calculates the electromagnetic fields by solving the Maxwell equations. The next module, called the Electron Energy Transport Module (EETM), calculates the electron density, electron temperature, electron energy distribution function and electron impact reaction rates with a Monte Carlo procedure or with the Boltzmann equation, based on the electromagnetic fields calculated in the EMM. From these electron impact reaction rates, the third module, called the Fluid Kinetics Simulation (FKS) computes the heavy particle densities and fluxes by means of continuity equations, and the electrostatic field by means of Poisson's equation. This electrostatic field is used as input again in the EMM and a cycle through these three main modules is iterated until convergence.

An optional module, called the Plasma Chemistry Monte Carlo simulation (PCMCS), is used to calculate plasma species fluxes and energy distributions to the substrate to produce detailed information at the substrate level. In addition, an analytical module within this hybrid code is addressed to predict the etch rate based on the calculated fluxes and kinetic energies of the different plasma species arriving at the silicon wafer. The reaction sets describing the plasma and surface

chemistries are identical to those described in our previous work for a HBr/He plasma[21] and are not repeated here, except for the reactions concerning $HBr^{(vib)}$, which are listed in **Table 1**, as well as the corresponding threshold energies and references where the cross sections are adopted from. We included three vibrational states, with energies of 0.3, 0.6 and 0.9 eV. Hence, three different electron impact excitations, with different thresholds, are included (first reaction in **Table 1**), as well as three different electron impact dissociation reactions from these vibrational levels (fourth reaction). The second reaction denotes electron impact excitation from the lowest vibrational levels to the two higher levels. For the other reactions, i.e., the quenching of $HBr^{(vib)}$ to HBr (third reaction in **Table 1**), the dissociative attachment of $HBr^{(vib)}$, and the ionization of $HBr^{(vib)}$ (i.e., last two reactions in **Table 1**), the three states are lumped into one species. Hence, for these reactions only one cross section is used.

Table 1. Reactions concerning $HBr^{(vib)}$ included in the model. All other reactions are described in our previous work.[22]

Reaction	Threshold (eV)	Reference
$e + HBr \rightarrow HBr^{(vib)} + e$	0.3/0.6/0.9	[18]
$e + HBr^{(vib)} \rightarrow HBr^{(vib)} + e$	0.31/0.58	[18]
$e + HBr^{(vib)} \rightarrow HBr + e$	-0.3	[24]
$e + HBr^{(vib)} \rightarrow Br + H + e$	4.34/6.6/9.3	[18]
$e + HBr^{(vib)} \rightarrow Br^{-} + H$	0.08	[19]
$e + HBr^{(vib)} \rightarrow HBr^{+} + e + e$	12.74	[24]

3. Results and discussion

Calculations are performed with and without $HBr^{(vib)}$ for the following operating conditions: ICP coil power of 800 W operated at 13.56 MHz, 60 mTorr chamber pressure, 100 sccm total gas flow rate with He fraction varied from 1% to 99%, and a 13.56 MHz radio frequency voltage applied at the substrate electrode generating a dc -200 V bias. The two-dimensional simplified reactor geometry resembles that of an industrial Lam Research 2300 Versys Kyo transformer coupled plasma (TCP), as shown in **Figure 2**.[25] The substrate is defined as a blanket silicon wafer (i.e., 100% Si).

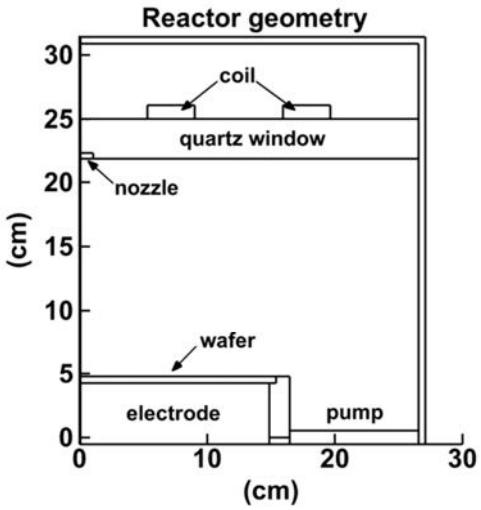

Figure 2. Two-dimensional reactor geometry defined in the model, based on the industrial Lam Research 2300 Versys Kyo ICP etch reactor.[25]

The calculated volume averaged densities of ground state HBr and $HBr^{(vib)}$ as a function of He gas fraction, for both simulations with and without $HBr^{(vib)}$, are presented in **Figure 3a**. The densities of the most important plasma species for silicon etching (i.e., H, Br and the total positive ion density), as well as the Br^- ion and electron density, are separately shown in **Figure 3b** for clarity.

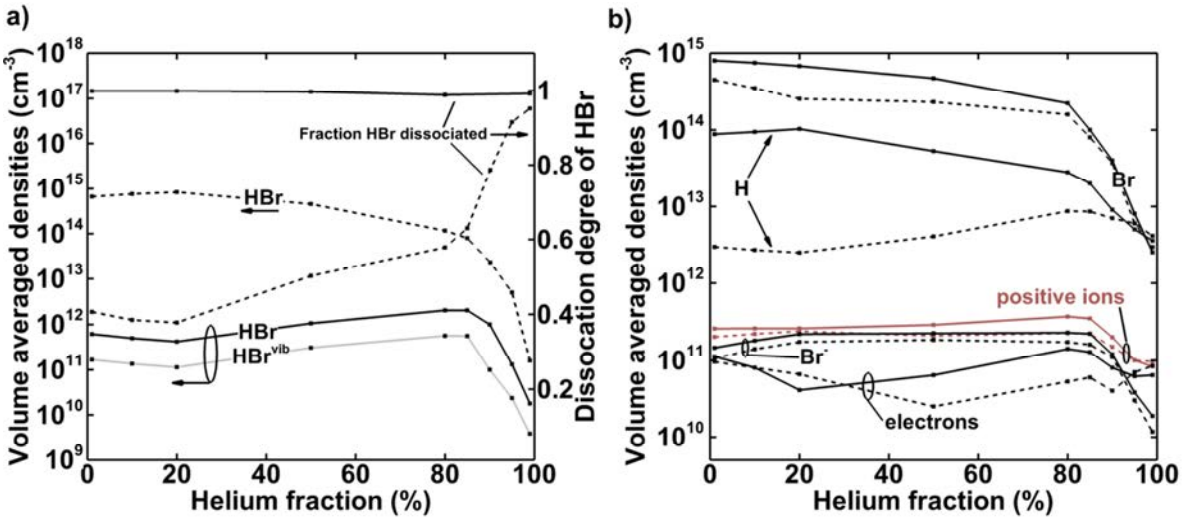

Figure 3. Calculated volume averaged densities of ground state HBr and $HBr^{(vib)}$ (left axis) and the fraction of HBr dissociated in the plasma (right axis) (a); as well as the H, Br, Br^-, electron and total positive ion density (b), as a function of He gas fraction, for both simulations with $HBr^{(vib)}$ (solid lines) and without $HBr^{(vib)}$ (dashed lines).

The difference in dissociation degree of the HBr feed gas with and without inclusion of $HBr^{(vib)}$ in the calculation is tremendous. Without vibrational excitation, the dissociation degree of HBr is already quite large, i.e., 40-95%, depending on the He fraction, but in the case with $HBr^{(vib)}$, always more than 99% is dissociated. In the latter case, about 10% of all HBr is vibrationally excited (see **Figure 3a**). Thus, HBr is rapidly converted to $HBr^{(vib)}$ when it is inserted from the nozzle, upon which it also rapidly dissociates into H + Br, and especially into H + Br^-, because of the much lower threshold for dissociative attachment than for direct dissociation (see **Table 1** in section 2). As a consequence, a large amount of the important etching species, H and Br, originate from dissociation of $HBr^{(vib)}$. The HBr/He plasma appears always to be electronegative, except at high He fractions (i.e., >90%), where the formation of Br^- is limited due to the low HBr gas fraction. Due to the easier dissociative attachment of $HBr^{(vib)}$ compared to ground state HBr (see cross sections in **Figure 1** in section 1), Br^- is about 25-40% more abundant when $HBr^{(vib)}$ is included. However, a large fraction of Br^- ions are neutralized through ion-ion neutralizations and electron impact detachment, explaining the much higher Br density vs. Br^- ion density.

When HBr^{vib} is not considered, the dissociation degree of HBr increases along with the He fraction as can be seen from **Figure 3a**. This is due to the fact that the thresholds for ionization and electronic excitation of He are much higher than those of HBr (i.e., 19.80 eV and 21.20 eV for excitation of He; 24.58 eV for ionization of He; compared to 4.34 eV for dissociation of HBr, and 12.74 eV for ionization of HBr). Thus, at higher He fractions, low threshold reactions become near absent, which results in a facilitated buildup of electron energy and average electron temperature. As a result, the higher average electron temperature allows for more dissociations of HBr molecules.

When HBr^{vib} is included in the model, the dissociation degree of HBr is very high (i.e., > 99%) for the entire range of He/HBr gas mixing ratios; it only slightly decreases upon increasing He fraction as can be seen from **Figure 3a**. The reason is again the increase in the average electron temperature (as shown in **Figure 4** below). With HBr^{vib} included, the main dissociation process for HBr is through dissociation of HBr^{vib}. This reaction has a much higher cross section and is therefore the dominant loss process of HBr (see **Figure 1** above). The rate of this reaction, however, quickly drops upon increasing electron temperature. As a result, the most important dissociative process for

HBr becomes gradually less important at higher He fractions. However, as shown in **Figure 3a**, the effect is minor, and the HBr dissociation degree in this case is always close to 100%.

The total number of positive ions in the plasma is not so much affected by incorporating $HBr^{(vib)}$ in the model. These ions are mostly created through electron impact ionization processes, which have relatively high thresholds. The total number of positive ions created thus depends strongly on the electron temperature, which is only slightly higher when $HBr^{(vib)}$ is included, as illustrated in **Figure 4**. Moreover, the total positive ion density tends to stay more or less constant as a function of He content. This is the result of two effects. The electron temperature increases with He fraction (see below), which will create more ions, but at the same time the ionization probability will drop, because of the higher ionization potential of He compared to HBr, and these two competing effects result in a fairly constant total positive ion density, except above 80% He, where the effect of the He fraction (and thus higher ionization potential) becomes dominant.

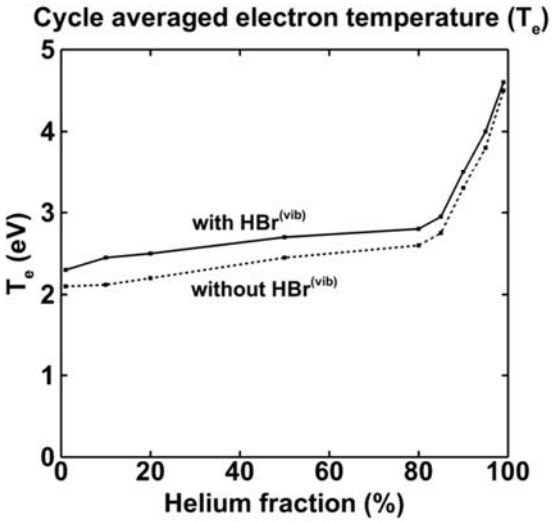

Figure 4. Calculated rf cycle averaged electron temperature as a function of He fraction, with $HBr^{(vib)}$ (solid line) and without $HBr^{(vib)}$ (dashed line).

As mentioned above, the electron temperature increases with He fraction (see **Figure 4**). The reason is that the gas mixture becomes more and more atomic, reducing the possibility of low-threshold reactions like vibrational and rotational excitations, which lower the average electron temperature. The electron temperature is also slightly (about 0.2 eV) higher with $HBr^{(vib)}$ included. This might be unexpected at first sight, because the frequent low-threshold vibrational excitations

should lower the electron energy significantly. However, as mentioned earlier, the fast vibrational excitation of HBr, followed by the even faster dissociative attachment of $HBr^{(vib)}$, results in almost total dissociation of the HBr gas within the reactor volume. Hence, the plasma is also much more atomic when $HBr^{(vib)}$ is included in the calculation, resulting in a slightly higher electron temperature, similar to the effect observed with increasing He fraction. The calculated average gas temperature is also about 50 K higher when vibrational excitation is included in the model, as appears from **Figure 5**.

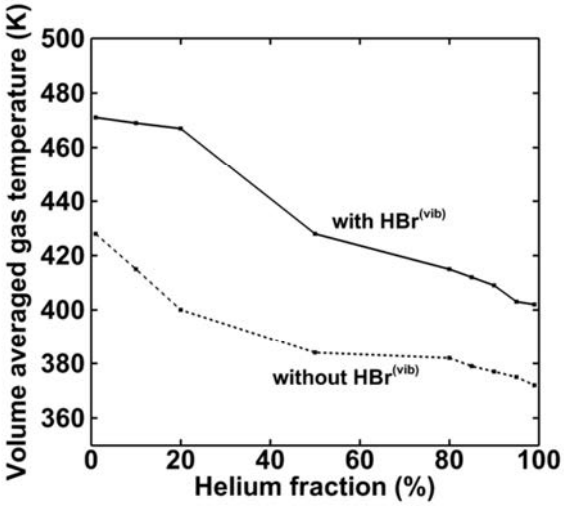

Figure 5. Calculated average gas temperature as a function of He fraction, with $HBr^{(vib)}$ (solid line) and without $HBr^{(vib)}$ (dashed line).

The most important heating mechanisms in this type of plasma are: (i) elastic collisions with energetic ions, (ii) charge exchange reactions, and especially (iii) Franck-Condon heating, as a result of electron impact dissociation, where the remaining energy is dissipated among the dissociation products.[26] With the inclusion of $HBr^{(vib)}$, dissociation becomes more prominent, as mentioned earlier, resulting in the formation of more high-temperature dissociation products (i.e., H and Br atoms) and thus in a higher overall gas temperature. For the same reason, the gas temperature decreases with He fraction, since the feed gas mixture becomes more atomic, reducing the amount of dissociation and thus Franck-Condon heating. The significantly higher density of H and Br in the plasma makes that the rate of chemical etching is about 3 times higher when $HBr^{(vib)}$ is included in the model, as is clear from

Figure 6. The difference becomes smaller when more He is added to the mixture, because of the decreasing role of chemical etching and the increasing role of physical sputtering by He^+ ions.

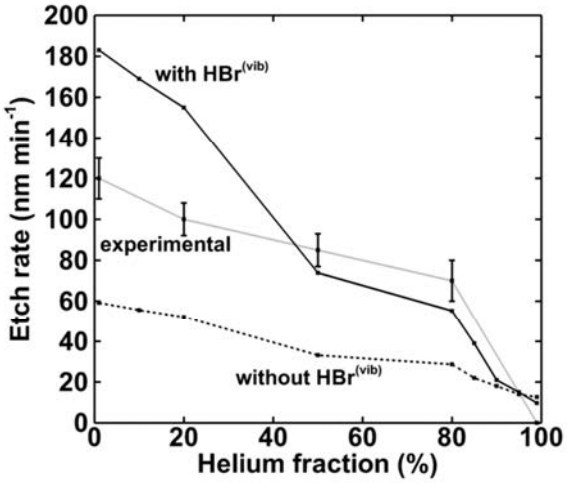

Figure 6. Calculated etch rates in the center of the wafer as a function of He fraction, with $HBr^{(vib)}$ (solid line) and without $HBr^{(vib)}$ (dashed line), compared with the experimentally measured etch rate from previous work.[21]

The experimentally measured etch rate drops from 120 nm min^{-1} in pure HBr to a rate near zero in pure He. The etch rate is definitely dependent on ion bombardment[1], but since the ion flux is more or less constant as a function of He fraction, it is clear that the chemical etching, especially by Br atoms, also plays a significant role (see **Figure 3b**; note that the flux towards the wafer is strongly correlated to the density in the plasma, so it shows a similar trend). Our model captures this trend properly, although the effect of chemical etching seems slightly overestimated in our model, explaining the more pronounced drop in our simulation results compared to the experimental data. The chemical composition on the surface during etching is practically identical with and without the inclusion of $HBr^{(vib)}$, as seen in **Figure 7**.

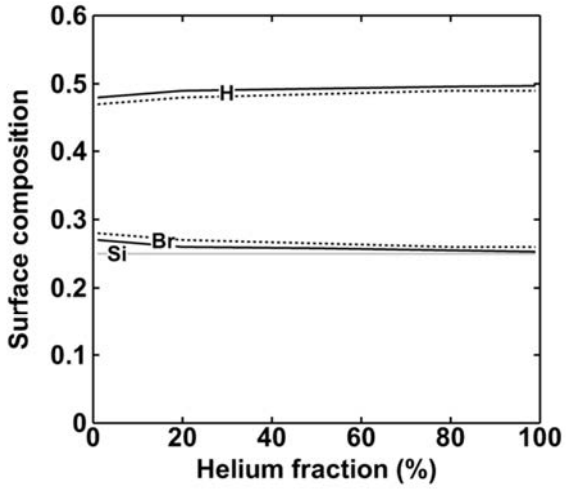

Figure 7. Calculated chemical composition of the wafer as a function of He fraction, with $HBr^{(vib)}$ (solid line) and without $HBr^{(vib)}$ (dashed line). The silicon content is identical in both cases and presented as the gray line.

The most chemically reactive species on silicon in the HBr/He plasma are the H atoms and Br atoms. The overall chemical composition of the wafer surface will thus depend on the ratio between the H and Br fluxes. Without $HBr^{(vib)}$, the flux of H atoms is about two orders of magnitude lower than the Br flux (see **Figure 3b**), but as H has a higher sticking probability than Br (e.g., 0.60 for H on SiHBr, compared to 0.20 for Br on SiHBr)[21], this results in a chemical composition of $SiH_{1.92}Br_{1.08}$. With $HBr^{(vib)}$ included in the model, the H flux is only about one order of magnitude lower than the Br flux, so we could expect a higher fraction of H and a lower fraction of Br on the surface. However, the chemical composition here is calculated as $SiH_{1.96}Br_{1.04}$, which is only marginally different. This indicates that the sticking probabilities are the decisive factor in determining the chemical composition of the surface, and not the fluxes, under these conditions.

4. Conclusions

We investigated the importance of including vibrationally excited HBr (i.e., $HBr^{(vib)}$) in modeling a HBr/He ICP used for Si etching. At least 50% of the total fraction of HBr feed gas that is dissociated in the plasma, originates from vibrational excitation of HBr, followed by electron impact dissociative

attachment and dissociation, rather than from direct electron impact dissociative attachment and dissociation of ground state HBr.

Because dissociative attachment of $HBr^{(vib)}$ is the most important process for creating H and Br products, including $HBr^{(vib)}$ in the model causes the plasma to become more atomic, resulting in a slightly higher electron temperature. Moreover, the gas temperature also becomes slightly higher, due to the important role of Franck-Condon heating, where HBr, and especially $HBr^{(vib)}$, become dissociated into "hot" products by electron impact.

The most chemically reactive species in the HBr/He plasma are H and Br atoms, and since these species are largely created by dissociation of $HBr^{(vib)}$, including $HBr^{(vib)}$ in the model results in a 3 times higher etch rate, compared to the model results where vibrational excitations of HBr are neglected. The calculated etch rate as a function of He fraction is in reasonable agreement with experimental data.

Finally, the calculated chemical composition of the wafer surface during etching is not affected by the presence of $HBr^{(vib)}$ in the model, which indicates that it is determined by the sticking coefficients of H and Br, rather than by the ratio between the fluxes of these species.

In general, we may conclude that vibrationally excited HBr definitely should be included in modeling HBr-containing mixtures in an ICP, as it largely affects the calculation results, especially the dissociation degree of HBr, and thus the densities and fluxes of HBr, H and Br atoms, and consequently also the Si etch rate. The same is most likely true for the other hydrogen halides like HCl.[18]

5. Acknowledgements

The Fund for Scientific Research Flanders (FWO) is acknowledged for financial support of this work (Grant no. 0880.212.840). This work was carried out in part using the Turing HPC infrastructure at the CalcUA core facility of the Universiteit Antwerpen, a division of the Flemish Supercomputer Center VSC, funded by the Hercules Foundation, the Flemish Government (department EWI) and the

University of Antwerp. Prof. Mark Kushner is also gratefully acknowledged for the useful discussions and for providing the HPEM code.

6. References

[1] Donnely V and Kornblit A, *J. Vac. Sci. Technol. A* **31** 050825 (2013)

[2] Hayashi T, Ishikawa K, Sekine M and Hori M, *Jap. J. appl. phys.* **54** 06GA03 (2015)

[3] Haass M, Darnon, M, Cunge G, Joubert O and Gahan D, *J. Vac. Sci. Technol. B* **33** 032202 2015

[4] Haass M, Darnon, M, Cunge G, Joubert O and Gahan D, *J. Vac. Sci. Technol. B* **33** 032203 2015

[5] Berg A, Mergenthaler K, Ek M, Pistol M, Wallenberg L and Borgström M, *Nanotechnology* **25** 505601 (2014)

[6] Sirse N, Foucher M, Chabert P and Booth P, *Plasma Sources Sci. Technol. B* **23** 062003 (2014)

[7] Zhu W, Sridhar S, Liu L, Hernandez E, Donnelly V and Economou D, *J. Appl. Phys.* **115** 203303 (2014)

[8] Cunge G, Inglebert R, Joubert O, Vallier L and Sadeghi N, *J. Vac. Sci. Technol. B* **20** 2137 (2002)

[9] Srivastava A, Ohashi T and Donnelly V, *J. Vac. Sci. Technol. A* **33** 041301 (2015)

[10] Tseng Y and Tsui B, *J. Vac. Sci. Technol. A* **32** 031601 (2014)

[11] Suzuki E, Ohtake H, Ohsawa Y, Kumar K and Sasaki M, *Jap. J. Appl. Phys.* **53** 03DD01 (2014)

[12] Park W, Lee W, Kim W, Kim H and Whang K, W. *Jap. J. Appl. Phys.* **53** 036502 (2014)

[13] Iino D, Nojiri, Y, Suzuki K, Oike T, Fujii Y and Toyoda, H, *J. Appl. Phys.* **52** 11NC01 (2013)

[14] Kwon K, Efremov A, Kim M, Min N, Jeong J and Kim K, *J. Electrochem. Soc.* **157** H574 (2010)

[15] Kim D, Kim Y and Lee H, *Mat. Sci. Sem. Proc.* **10** 41 (2007)

[16] Delalande M, Cunge G, Chevolleau T, Bézard P, Archambault S, Joubert O and Tiron R, *J. Vac. Sci. Technol. B* **32** 051806 (2014)

[17] Fouchier M and Pargon E, *J. Appl. Phys.* **115** 074901 (2014)

[18] Bardsley J and Wadehra J, *J. Chem. Phys*. **78** 7227 (1983)

[19] Horacek J and Domcke W, *Phys. Review A* **53** 2262 (1996)

[20] Godyak V, Piejak R and Alexandrovich B, *Plasma Sources Sci. Technol.* **1** 36 (1992)

[21] Gul B, Tinck S, De Schepper P, Rehman A and Bogaerts A, *J. Phys. D: Appl. Phys*. **48** 025202 (2015)

[22] Efremov A, Kim J and Kwon K, *Plasma Chem. Plasma Process*. **35** 1129 (2015)

[23] Kushner M, *J. Phys. D Appl. Phys*. **42** 194013 (2009)

[24] W. L. Morgan, *"Electron Collision Data for Plasma Chemistry Modeling*: *Advances in Atomic, Molecular, and Optical Physics"*, Vol. 43, ISBN: 978-0-12-003843-5 (2000)

[25] Lam Research Corporation www.lamrc.com

[26] Agarwal A, Rauf S and Collins K, *Plasma Sources Sci. Technol*. **21** 055012 (2012)